



## RESEARCH ARTICLE

# Studying Hardness Meter Spring Strength to Understand Hardness Distribution on Body Surfaces



Yoshitaka Arima\*

Department of Acupuncture and Moxibustion Therapy, Faculty of Health Promotional Sciences,  
Tokoha University, Hamamatsu-shi, Shizuoka, Japan

Available online 12 August 2017

Received: Jun 15, 2017

Revised: Aug 4, 2017

Accepted: Aug 8, 2017

**KEYWORDS**

biological body surface;  
biological tissue  
hardness;  
breast cancer  
induration;  
hardness distribution;  
hardness meter

**Abstract**

**Introduction:** For developing a hardness multipoint measurement system for understanding hardness distribution on biological body surfaces, we investigated the spring strength of the contact portion main axis of a biological tissue hardness meter (product name: PEK).

**Methods:** We measured the hardness of three-layered sheets of six types of gel sheets (90 mm × 60 mm × 6 mm) constituting the acupuncture practice pads, with PEK measurements of 1.96 N, 2.94 N, 3.92 N, 4.90 N, 5.88 N, 6.86 N, 7.84 N, 8.82 N, and 9.81 N of the main axis spring strength. We obtained measurements 10 times for the gel sheets and simultaneously measured the load using a digital scale. We measured the hardness distribution of induration embedded and breast cancer palpation models, with a main axis with 1.96 N, 4.90 N, and 9.81 N spring strengths, to create a two-dimensional Contour Fill Chart.

**Results:** Using 4.90 N spring strength, we could obtain measurement loads of  $\leq 3.0$  N, and the mean hardness was 5.14 mm. This was close to the median of the total measurement range 0.0–10.0 mm, making the measurement range the largest for this spring strength. We could image the induration of the induration-embedded model regardless of the spring strength.

**Conclusion:** Overall, 4.90 N spring strength was best suited for imaging cancer in the breast cancer palpation model.

\* Corresponding author. Department of Acupuncture and Moxibustion Therapy, Faculty of Health Promotional Sciences, Tokoha University, 1230, Miyakoda-cho, Kita-ku, Hamamatsu-shi, Shizuoka 432-2102, Japan.

E-mail: [arima@hm.tokoha-u.ac.jp](mailto:arima@hm.tokoha-u.ac.jp).

pISSN 2005-2901 eISSN 2093-8152

<http://dx.doi.org/10.1016/j.jams.2017.08.001>

© 2017 Medical Association of Pharmacopuncture Institute, Publishing services by Elsevier B.V. This is an open access article under the CC BY-NC-ND license (<http://creativecommons.org/licenses/by-nc-nd/4.0/>).

## 1. Introduction

In acupuncture therapy, the therapist understands the pathologic condition using responses to stimulation applied to the body surface, which is also used as a therapeutic medium. The therapist focuses on information regarding pain or tenseness, which is required to correctly diagnose, treat, and estimate the effects of treatment. The therapist also focuses on information regarding hardness, such as induration, as well as on acupoints and trigger points. Trigger points that commonly overlap with acupuncture points [1,2] can be found as a lowered pressure pain threshold above a cord-like induration [3]. Also, in patients with chronic lower back pain, acupuncture to deep parts is considered to be more effective than acupuncture to superficial parts [4,5].

We used a system that seeks curve inclination  $\Delta P/\Delta L$  for each pressing distance,  $\Delta L$ , from the load–displacement relationship to find deep indurations. We exchanged sheets of varying hardness to measure the stratified compound tissues simulated by the model [6]. Comparison between models demonstrated that the reflection of deep-region hard sheets could be confirmed. However, comparison between measured sites demonstrated that the values did not correspond with sheet positions. Since superficial hardness has a structure dependence because it varies according to the hard structures in deeper regions, we concluded that detecting depth-dependent (vertical) differences in hardness using load–displacement measurement is difficult. Therefore, we decided to measure hardness on a flat surface (laterally) for measuring induration.

To find indurations by measuring lateral hardness on a flat surface, methods such as displaying results of measurements on multiple points on a two-dimensional (2D) Contour Fill Chart are used. The current method is time-consuming because it comprises the following steps. First, a lattice drawn on the body surface is used as a reference for the measured part, after which measurements are obtained, the measured values are read, recording is repeated, and finally, the results are entered into the computer for imaging. We are planning to develop a multipoint measurement system for hardness because we require a system that permits rapid multipoint measurement with high induration imaging capacity.

For measurement using the multipoint measurement device, we used the biological tissue hardness meter (PEK; Imoto Machinery Co., Ltd., Kyoto, Japan), which is commercially available in Japan and is a simplified pressing force-type hardness meter for biological body surfaces [7]. The measurement device PEK-1 is widely used in a several areas, such as dentistry [8,9]; alternative medicine, such as acupuncture or chiropractic treatments [10–12]; orthopedics, rehabilitation, and sports medicine [13–16]; industrial hygiene [17]; behavioral medicine [18]; basic animal experiments [19,20]; and for assessing the validity of other measurements of hardness [21]. A hardness index of PEK is the shift distance of the main axis (mm) when the auxiliary cylinder is shifted by 10.0 mm, and the contact force of main axis at the time of measurement affects hardness detection [6]. However, to our knowledge, to date, no study has focused on the spring strength of the main axis.

Thus, we used a model that simulated the hardness of biological soft tissues to study the differences in the detectability of hardness and indurations depending on the spring strength of the main axis.

## 2. Materials and methods

### 2.1. Spring strength and detection characteristics

For the hardness model, we used three-layered sheets of six types of silicon gels of various hardness (measuring approximately 90 mm × 60 mm × 6 mm; in order of soft to hard: SG-a, SG-b, SG-c, SG-d, SG-e, and SG-f) from the Unico acupuncture practice pads Type V (Nissin Medical Industries Co. Ltd., Kitanagoya, Japan), which are used in acupuncture education in Japan, layered on top of each other. For measuring hardness, we used a specially ordered model with an exchangeable main axis spring of the pressure pain PEK, which can measure the pressure pain threshold by continuing to press after measuring hardness, using the biological tissue hardness meter PEK-1 (Imoto Machinery Co., Ltd.). The main axis spring strength was adjusted to 1.96 N, 2.94 N, 3.92 N, 4.90 N, 5.88 N, 6.86 N, 7.84 N, 8.82 N, or 9.81 N (Fig. 1). The point of contact of the biological tissue hardness meter comprised the main axis and an auxiliary cylinder. The hardness index of 0–100 indicates the relative comparative value of 10 times the shift distance of the main axis (mm) when the auxiliary cylinder is shifted by 10 mm. The corners of the main axis are rounded so that the measured object is not damaged when measured at a 7-mm diameter. It is shaped like the brim of a hat with an external diameter of 25 mm and internal diameter of 14 mm to increase contact stability and pressing force for support. When measuring hard objects, the main axis and auxiliary cylinder shift in a uniform manner. The measured value increases in proportion to the increase in the main axis and auxiliary cylinder shift distance. For measuring soft objects, the shift distance of the main axis is smaller than that of the auxiliary cylinder; thus, the measured value is small (Fig. 1) [7,20]. For measuring the load, we used a digital cooking scale (KD-320; Tanita Co., Tokyo, Japan).

Measurements were obtained 10 times for the varying hardness of the six types of gels and varying spring strengths of the main axis for maximum load at measurement. We created a distribution chart by plotting mean values with standard deviations. We determined the skewness of the six types of gels and the range by subtracting the mean values of hardness of SG-a from those of SG-f to assess the detectability from the results of hardness. The ranges were also calculated in a similar manner from the results of the loads.

### 2.2. Expression of hardness distribution

We used the induration-embedded model (Nakamura Brace Co., Ltd., Omoricho Oda, Japan) and breast cancer palpation model (Kyoto Kagaku Co., Ltd., Kyoto, Japan) as the models of induration (Fig. 2). To a 140 mm × 140 mm × 40-mm silicone gel block, we embedded two types of hemispherical silicone of different hardness (A, a mixture of AskerC19 and silicone gel and B, addition of 50% JIS A40 and 50% AskerC19 to A and forming a 1-mm-thick coating) so

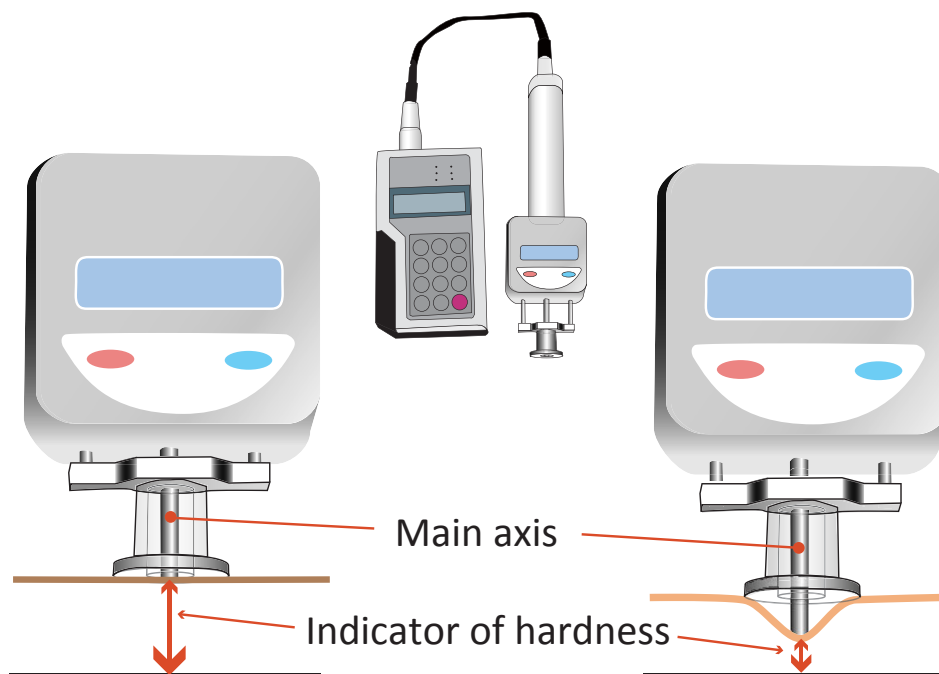


**Figure 1** Hardness meter and mechanism of assessment. The shift distance of the main axis when the auxiliary cylinder displaces 10 mm is used as the index of hardness.

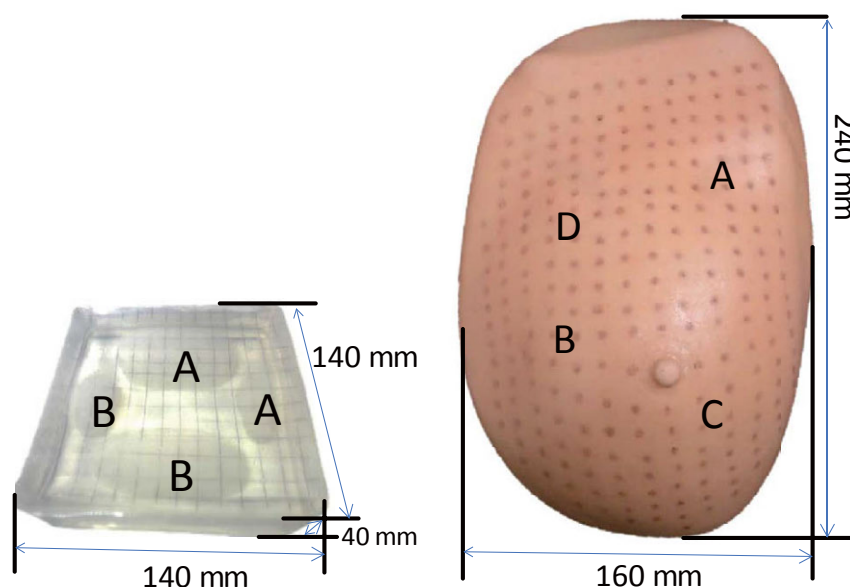


**Figure 2** Induration model. Left: induration-embedded model (A > B). Right: breast cancer palpation model (A, cancer accompanied by dimpling signs; B, cancer accompanied by depressed areas of the skin; C, fibroadenomas; and D, breast cancer).

that the apex of the hemispheres was positioned 5 mm from the surface. The soft special resin breast cancer palpation model measured approximately 240 mm × 160 mm × 60 mm and simulated the following: (1) cancer accompanied by dimpling signs; (2) cancer accompanied by depressed areas of the skin; (3) fibroadenomas; and (4) breast cancer.

We used the pressure pain PEK main axis with 1.96 N, 4.90 N, and 9.81 N spring strengths to measure the induration-embedded model at 156 (13 rows × 12 columns) points. The breast cancer palpation model was measured at 238 points distanced 10 mm from each other, and we created a 2D Contour Fill Chart using DeltaGraph5 (Red Rock Software, Inc., Salt Lake City, Utah, USA).

### 3. Results

#### 3.1. Spring strength and detection characteristics

At 4.90 N spring strength, the mean hardness was 5.14 mm, which was close to the median hardness for the full measured range of 0.0–10.0 mm. The range was widest at 5.65 mm and was  $\geq 5.00$  mm at 5.88 N, 6.86 N, and 9.81 N spring strengths (Fig. 3). The skewness reached 0 at 8.82 N and had the highest degree of symmetry; the skew to hard objects tended to increase for low spring strength. From the points of the plot on the graph, we can deduce that  $\geq 3.92$  N spring strengths are required for discriminating among SG-d, SG-e, and SG-f.

For adequate measurement, as the spring strength decreased, lower and more constant load was required during measurement (Fig. 4). The means at 1.96 N and 9.81 N spring strengths were 3.44 N and 5.80 N. Thus, within this range, the load increased in proportionate to spring strength intensity. Although the range for 4.90 N spring strength was 2.66 N, the range increased to 3.84 N after spring strength was increased to  $\geq 5.88$  N. In other words, the range tended to widen as the intensity increased.

#### 3.2. Expression of hardness distribution

The 2D Contour Fill Chart of the induration-embedded and breast cancer palpation models is imaged for the hardness range of 4.0–10.0 mm for 1.96 N spring strength, of 2.0–8.0 mm for 4.90 N spring strength, and of 0.0–6.0 for 9.81 N spring strength for comparison (Figs. 5 and 6). We could image the induration form of the induration-embedded model regardless of the spring strength, thereby allowing us to detect the difference in hardness (Fig. 5). In the breast cancer palpation model, we could not image any cancer for 9.21 N spring strength, fibroadenoma (Fig. 6C) could only be imaged for 1.96 N. For 4.90 N spring strength, cancer accompanied by depressed areas of the

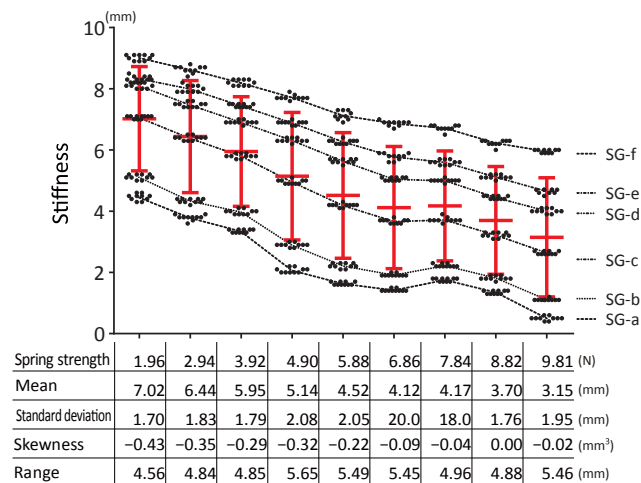


**Figure 3** Results of hardness measurement. The mean is 51.4 at 4.90 N spring strength, with the largest range. The skewness shows that the detectability lowers for weaker springs and harder objects.

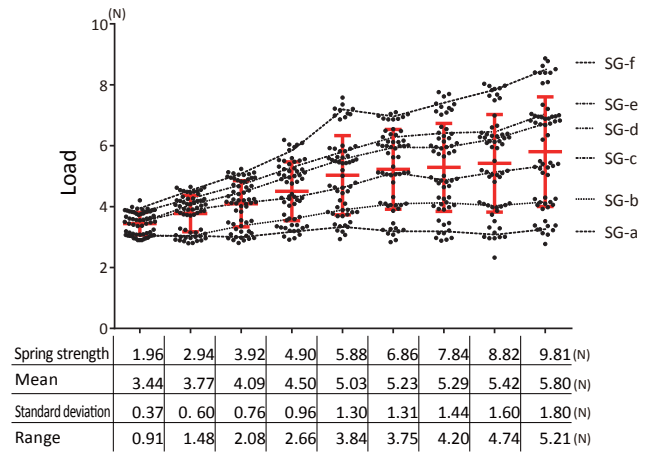


**Figure 4** Load during measurement. Weaker spring strength indicates that smaller and more constant load is required for measurement.

skin (Fig. 6B), fibroadenoma (Fig. 6C), and breast cancer (Fig. 6D) were rendered as areas harder than the surrounding tissues. Cancers accompanied by dimpling signs could not be imaged for any spring strength.

### 4. Discussion

The detectability of hard objects was lowered because the skews to hard objects from skewness values increased. Thus, we believe that  $\geq 3.92$  N spring strengths are required to measure hard objects. The silicone gels simulate the hardness of soft biological tissues that are used by Japanese acupuncturists while practicing acupuncture or palpation. Acupuncturists focus on soft tissues as reaction points in addition to tissues that are harder than the surrounding tissues on the body surface. For the objective assessment of hardness focused on clinical acupuncture, a spring strength of 4.90 N is one option because its mean lies within the median of 0.0–10.0 mm. A spring strength of 9.81 N also demonstrated a similar range of  $\geq 5.0$  mm, indicating that harder objects could also be measured. Therefore, intense spring strengths are another option to choose among those depending on the hardness range of the object. However, measurements with less force are ideal to reduce the level of invasion to the surface of the measured part. Because measurements can be obtained at relatively weak and safe loads of 3.00 N for spring strengths of up to 4.90 N, this may also be an important factor in selecting appropriate spring strength. Our results also suggested that for  $\geq 5.88$  N spring strengths, load during measurement, rather than distance, may also be an important indicator of hardness.

We could extract the internal silicone form with the hardness 2D Contour Fill Chart of the induration-embedded model regardless of spring strength, and thus, we could detect the difference in hardness. In contrast, in the breast cancer palpation model, we could not detect cancers accompanied by dimpling signs as hardness for any spring strength. Nonetheless, we could image cancers accompanied by depressed areas of skin, fibroadenoma, and breast cancer with a 4.90 N spring strength.

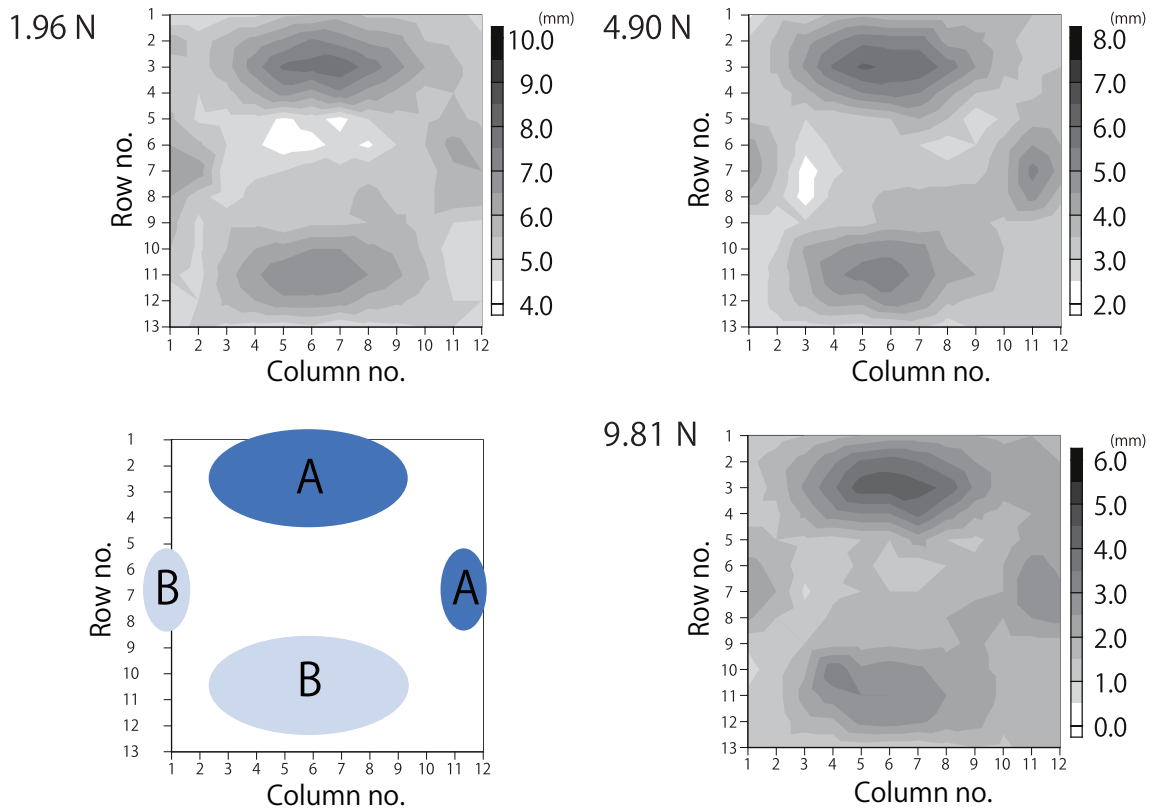


**Figure 5** The contour plan distribution chart of hardness of the induration-embedded model. The shape of the induration could be imaged and the difference in hardness could be detected regardless of the spring strength.

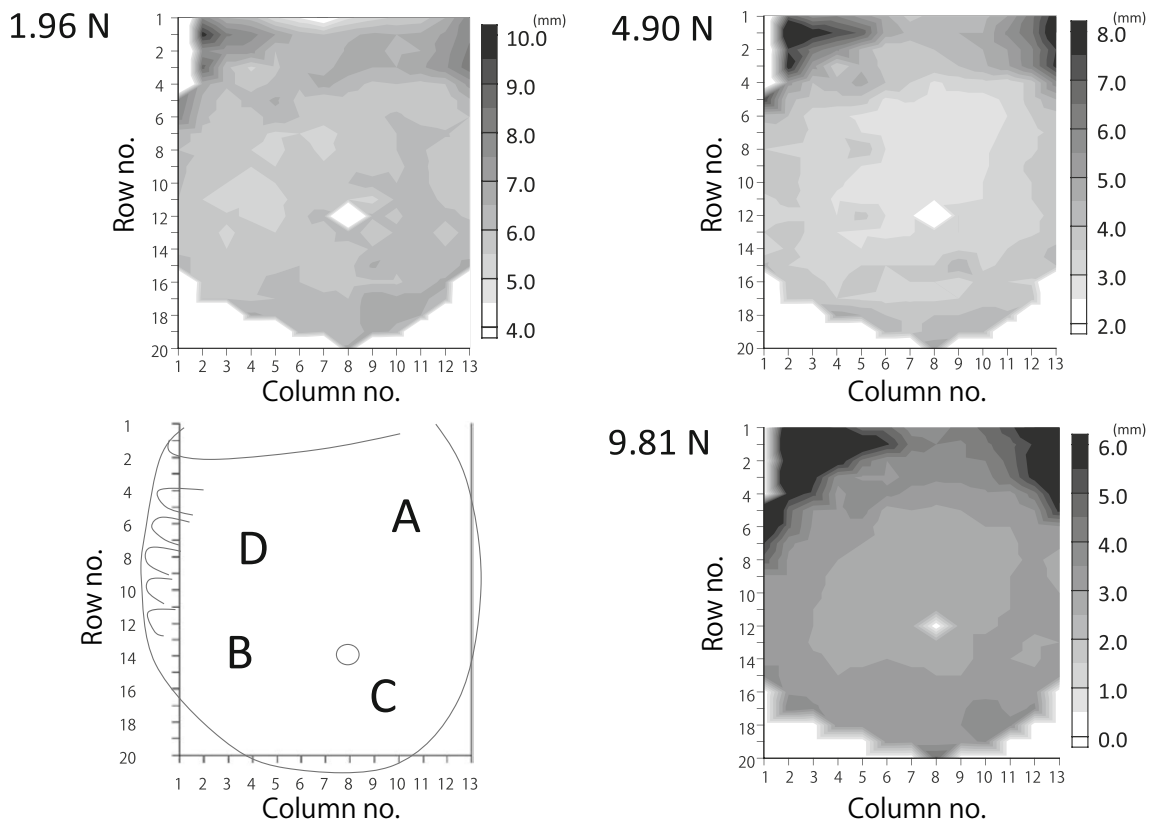


**Figure 6** Contour plan distribution chart of the hardness of the breast cancer palpation model. 1.96 N: C could be imaged. 4.90 N: B, C, and D could be imaged.

From the results of hardness detectability and deep induration imageability in hardness or induration models that simulated human biological soft tissues, we found that 4.90 N was the most versatile and suitable spring strength of the main axis of multipoint measurement systems for hardness.

## Disclosure statement

The author declare that he have no conflicts of interest and no financial interests related to the material in this manuscript.

## Acknowledgments

Dr Arima reports grants from JSPS KAKENHI (Grant Number C25460916) during the conduct of the study. The author thanks Crimson Interactive Pvt. Ltd. (Ulatius; [www.ulatus.jp](http://www.ulatus.jp)) for their assistance in manuscript translation and editing.

## References

- [1] Birch S. Trigger point—acupuncture point correlations revisited. *J Altern Complement Med.* 2003;9:91–103.
- [2] Melzack R, Stillwell DM, Fox EJ. Trigger points and acupuncture points for pain: correlations and implications. *Pain.* 1977; 3:3–23.
- [3] Itoh K, Okada K, Kawakita K. A proposed experimental model of myofascial trigger points in human muscle after slow eccentric exercise. *Acupunct Med.* 2004;22:2–13.
- [4] Ceccherelli F, Bordin M, Gagliardi G, Caravello MN. Comparison of superficial and deep acupuncture in the treatment of lumbar myofascial pain: a double-blind randomized controlled study. *Clin J Pain.* 2002;18(3):149–153.
- [5] Itoh K, Katsumi Y, Kitakoji H. Trigger point acupuncture treatment of chronic low back pain in elderly patients—a blinded RCT. *Acupunct Med.* 2004;22:170–177.
- [6] Arima Y, Yano T. Basic study on objectification of palpation [in Japanese]. *JJME.* 1998. <http://dx.doi.org/10.11239/jsmbe1963.36.321> [Date accessed: August 4, 2017].
- [7] Kato G, Andrew PD, Sato H. Reliability and validity of a device to measure muscle hardness. *J Mech Med Biol.* 2004;4: 213–225.
- [8] Kashima K, Igawa K, Maeda S, Sakoda S. Analysis of muscle hardness in patients with masticatory myofascial pain. *J Oral Maxillofac Surg.* 2006;64:175–179.
- [9] Kashima K, Higashinaka S, Watanabe N, Maeda S, Shiba R. Muscle hardness characteristics of the masseter muscle after repetitive muscle activation: comparison to the biceps brachii muscle. *CRANIO.* 2004;2:276–282.
- [10] Matsubara T, Arai YC, Shiro Y, Shimo K, Nishihara M, Sato J, et al. Comparative effects of acupressure at local and distal acupuncture points on pain conditions and autonomic function in females with chronic neck pain. *Evid Based Complement Alternat Med.* 2011. <http://dx.doi.org/10.1155/2011/543291> [Date accessed: August 4, 2017].
- [11] Ogura T, Tashiro M, Masuda M, Watanuki S, Shibuya K, Itoh M, et al. Cerebral metabolic changes in men after chiropractic spinal manipulation for neck pain. *Altern Ther Health Med.* 2011;6:17.
- [12] Inami A, Ogura T, Watanuki S, Masud MM, Shibuya K, Miyake M, et al. Glucose metabolic changes in the brain and muscles of patients with nonspecific neck pain treated by spinal manipulation therapy: a [<sup>18</sup>F] FDG PET Study. *Evid Based Complement Alternat Med.* 2017. <http://dx.doi.org/10.1155/2017/4345703> [Date accessed: August 4, 2017].
- [13] Sun G, Miyakawa S, Kinoshita H, Shiraki H, Mukai N, Takemura M, et al. Changes in muscle hardness and electromyographic response for quadriceps muscle during repetitive maximal isokinetic knee extension exercise. *Football Sci.* 2009; 6:17–23. <http://www.shobix.co.jp/jssf/tempfiles/journal/2009/028.pdf> [Date accessed: August 4, 2017].
- [14] Takahashi J, Ishihara K, Aoki J. Effect of aqua exercise on recovery of lower limb muscles after downhill running. *J Sports Sci.* 2006;24:835–842.
- [15] Nakano S, Wada C. Influence of electrical stimulation on hip joint adductor muscle activity during maximum effort. *J Phys Ther Sci.* 2016;28:1633–1635.
- [16] Kinoshita H, Miyakawa S, Mukai N, Kono I. Measurement of tissue hardness for evaluating flexibility of the knee extensor mechanism. *Football Sci.* 2006;3:15–20. <http://www.shobix.co.jp/jssf/tempfiles/journal/2006/015.pdf> [Date accessed: August 4, 2017].
- [17] Matsumoto H, Takenami E, Iwasaki-Kurashige K, Osada T, Katsumura T, Hamaoka T. Effects of blackcurrant anthocyanin intake on peripheral muscle circulation during typing work in humans. *Eur J Appl Physiol.* 2005;94:36–45.
- [18] Nakaya N, Kumano H, Minoda K, Kanazawa M, Fukudo S. Laterality and imbalance of muscle stiffness relate to personality. *Behav Med.* 2004;1:30.
- [19] Hayashi K, Ozaki N, Kawakita K, Itoh K, Mizumura K, Furukawa K. Involvement of NGF in the rat model of persistent muscle pain associated with taut band. *J Pain.* 2011;12: 1059–1068.
- [20] Morisada M, Okada K, Kawakita K. Quantitative analysis of muscle hardness in tetanic contractions induced by electrical stimulation in rats. *Eur J Appl Physiol.* 2006;97:681–686.
- [21] Yanagisawa O, Niitsu M, Kurihara T, Fukubayashi T. Evaluation of human muscle hardness after dynamic exercise with ultrasound real-time tissue elastography: a feasibility study. *Clin Radiol.* 2011;66:815–819.